



## Tuning color variation in grape anthocyanins at the molecular scale.

Laura Rustioni, Florent Di Meo, Maxime Guillame, Osvaldo Failla, Patrick Trouillas

### ► To cite this version:

Laura Rustioni, Florent Di Meo, Maxime Guillame, Osvaldo Failla, Patrick Trouillas. Tuning color variation in grape anthocyanins at the molecular scale.. Food Chemistry, 2013, 141 (4), pp.4349-57. 10.1016/j.foodchem.2013.07.006 . inserm-00845052

**HAL Id: inserm-00845052**

**<https://www.hal.inserm.fr/inserm-00845052>**

Submitted on 16 May 2014

**HAL** is a multi-disciplinary open access archive for the deposit and dissemination of scientific research documents, whether they are published or not. The documents may come from teaching and research institutions in France or abroad, or from public or private research centers.

L'archive ouverte pluridisciplinaire **HAL**, est destinée au dépôt et à la diffusion de documents scientifiques de niveau recherche, publiés ou non, émanant des établissements d'enseignement et de recherche français ou étrangers, des laboratoires publics ou privés.

## Accepted Manuscript

### Tuning Color Variation In Grape Anthocyanins At The Molecular Scale

Laura Rustioni, Florent Di Meo, Maxime Guillaume, Osvaldo Failla, Patrick Trouillas

PII: S0308-8146(13)00927-8  
DOI: <http://dx.doi.org/10.1016/j.foodchem.2013.07.006>  
Reference: FOCH 14349

To appear in: *Food Chemistry*

Received Date: 23 April 2013  
Revised Date: 28 June 2013  
Accepted Date: 1 July 2013



Please cite this article as: Rustioni, L., Di Meo, F., Guillaume, M., Failla, O., Trouillas, P., Tuning Color Variation In Grape Anthocyanins At The Molecular Scale, *Food Chemistry* (2013), doi: <http://dx.doi.org/10.1016/j.foodchem.2013.07.006>

This is a PDF file of an unedited manuscript that has been accepted for publication. As a service to our customers we are providing this early version of the manuscript. The manuscript will undergo copyediting, typesetting, and review of the resulting proof before it is published in its final form. Please note that during the production process errors may be discovered which could affect the content, and all legal disclaimers that apply to the journal pertain.

# Tuning Color Variation In Grape Anthocyanins At The Molecular Scale

Laura Rustioni,<sup>a,b,\*</sup> Florent Di Meo,<sup>b</sup> Maxime Guillaume,<sup>c</sup> Osvaldo Failla<sup>a</sup>, Patrick

Trouillas<sup>b,c,d</sup>

<sup>a</sup> Università degli Studi di Milano, CIRIVE – Centro Interdipartimentale di ricerca per l'innovazione in Viticoltura ed Enologia, via Celoria 2, I-20133 Milano, Italy

<sup>b</sup> Inserm, UMR-S850, Faculté de Pharmacie, Université de Limoges, 2 rue du Dr Marcland, 87000 Limoges, France

<sup>c</sup> Laboratoire de Chimie des Matériaux Nouveaux, Université de Mons, Place du Parc, 20, B-7000, Mons, Belgium

<sup>d</sup> Regional Center of Advanced Technologies and Materials, Department of Physical Chemistry, Faculty of Science, Palacký University, 17. listopadu 1192/12, 77146 Olomouc, Czech Republic

## E-mail addresses:

[laura.rustioni@unimi.it](mailto:laura.rustioni@unimi.it), [florent.di-meo@unilim.fr](mailto:florent.di-meo@unilim.fr), [maxime.guillaume@umons.ac.be](mailto:maxime.guillaume@umons.ac.be),  
[osvaldo.failla@unimi.it](mailto:osvaldo.failla@unimi.it), [patrick.trouillas@unilim.fr](mailto:patrick.trouillas@unilim.fr)

## Corresponding author:

Università degli Studi di Milano

CIRIVE Centro Interdipartimentale di ricerca per l'innovazione in Viticoltura ed Enologia

via Celoria 2

I-20133 Milano

ITALY

Tel.: +390250316556

Fax: +390250316553

E-mail: [laura.rustioni@unimi.it](mailto:laura.rustioni@unimi.it)

34 **ABSTRACT**

35 Anthocyanins are the main grape pigments. Due to their aromatic cyclic arrangements, they  
36 are able to absorb the radiation in the low energy range of the visible spectrum. In the fruit of  
37 *Vitis vinifera* L., the five main anthocyanidins (cyanidin, peonidin, delphinidin, petunidin and  
38 malvidin) are present as 3-*O*-glucosides, as well as their acetyl, *p*-coumaroyl and caffeoyl  
39 ester forms. Despite the huge number of experimental studies dedicated to the anthocyanin  
40 profile analysis of grapes and wines, the complete theoretical elucidation of the optical  
41 properties of grape anthocyanins is missing. The present work carried out this task through  
42 quantum chemistry calculations based on time-dependent density functional theory (TD-  
43 DFT), compared to experimental spectra. The differences in visible absorption spectra  
44 between the most common grape anthocyanins were rationalized according to B-ring  
45 substitution, glucosylation and esterification. A particular attention was given to the intra-  
46 molecular copigmentation effect, demonstrating the existence of an intra-molecular charge  
47 transfer excited state for the *p*-coumaroyl and caffeoyl ester forms.

48  
49 **KEYWORDS:** UV/Vis absorption, intra-molecular copigmentation, optical properties,  
50 pigment profile, TD-DFT, grape anthocyanins, wine

51

## 52 INTRODUCTION

53 Anthocyanins are a class of  $\pi$ -conjugated compounds belonging to polyphenols. They are  
54 glycosides of the so-called anthocyanidins, characterized by a flavylium (2-phenyl-  
55 benzylpyrilium) skeleton (Fig. 1). The many possible chemical substitutions (with *e.g.*, OH  
56 and OMe groups) allow a large variety of compounds. They are pigments responsible for the  
57 shiny orange, pink, red, violet and blue colors in roots, stems, flowers and fruit of many plants  
58 (*e.g.*, orchids, grapes) (Castañeda-Ovando, Pacheco-Hernández, Páez-Hernández, Rodríguez  
59 & Galán-Vidal, 2009). Such a color variety is mainly driven by the capacity of these  
60 compounds to absorb green light (at around 520 nm), which has generally been attributed to  
61 the resonant structure of the flavylium cation (Allen, 1998; Castañeda-Ovando, et al., 2009).  
62 This was confirmed by quantum chemistry calculations, showing a highly delocalized  $\pi$ -  
63 conjugated system, spread over the entire molecule (Di Meo, Sancho Garcia, Dangles &  
64 Trouillas, 2012). This extended  $\pi$ -conjugation allows light absorption in the visible range  
65 rather than the violet to ultraviolet regions as it is described and theoretically rationalized for  
66 most of the other natural polyphenols (Anouar, Gierschner, Duroux & Trouillas, 2012).  
67 A thorough understanding of optical properties and pigmentation variation has become crucial  
68 in various domains including food and wine chemistry. We believe that in a near future  
69 fundamental rationalization of grape pigments should become mandatory to supporting the  
70 development of fast and non-invasive phenotyping strategies (Rustioni, Basilico, Fiori, Leoni,  
71 Maghradze & Failla, 2013). In grapes and wines, five anthocyanidin moieties are present in  
72 their glucosylated form, namely peonidin, cyanidin, malvidin, petunidin and delphinidin (Fig.  
73 1a). The most common anthocyanin in *Vitis vinifera* L. (*i.e.*, the common wine grape specie)  
74 is malvidin-3-*O*-glucoside (Kennedy, Saucier & Glories, 2006). There also exist anthocyanins  
75 having their glucose moiety attached to a carboxylic acid (acetic, *p*-coumaric and caffeic acids  
76 in *Vitis vinifera* L.) by an ester bond, giving rise to a group of acylated pigments (Fig. 1b)

(Allen, 1998). In the latter structures, intra-molecular copigmentation effects have been suggested (Dangles, Saito & Brouillard, 1993).

Despite all the available experimental studies focusing on the grape and wine anthocyanin profiles (Dallas & Laureano, 1994; Ferrandino, Guidoni & Mannini, 2007; Fischer, Löchner & Wolz, 2006; García-Puente Rivas, Alcalde-Eon, Santos-Buelga, Rivas-Gonzalo & Escribano-Bailón, 2006; Mattivi, Guzzon, Vrhovsek, Stefanini & Velasco, 2006; Roggero, Coen & Ragonnet, 1986; Rustioni, Rossoni, Calatroni & Failla, 2011; Rustioni, Rossoni, Cola, Mariani & Failla, 2011; Rustioni, Rossoni, Failla & Scienza, 2013), a profound understanding of the optical variability of these compounds is still missing. Quantum chemistry calculation is an adapted tool for investigation of these properties. In particular time dependent density functional theory (TD-DFT) enables to accurately characterize excited states and evaluate the subsequent absorption properties in the visible range. More than providing accurate absorption wavelengths, TD-DFT calculations provide a complete description of the excited states and thus allow full assignment of electronic transitions from the  $\pi$  to  $\pi^*$  molecular orbitals (MO) responsible for each UV/Vis absorption band. In this way, the method supports the tuning of pigmentation in various industrial applications e.g., pigment painting and solar cells. Moreover the intra-molecular interactions suggested from experience (Dangles, et al., 1993) can now be accurately evaluated by quantum calculations; these interactions are known to be responsible for copigmentation, but the process was only recently fully understood using dispersion-corrected DFT (DFT-D) calculations (Di Meo, et al., 2012).

The present work aims at rationalizing the differences in the absorption spectra between a series of grape anthocyanins, which has not been performed yet for these compounds. The series studied here is constituted of five glucosylated (compounds **1-5** in Figure 1a) and three acylated anthocyanins (compounds **6-8** in Figure 1b), which were investigated due to their

high occurrence in grape. This comprehensive study allows establishing a thorough structure-property relationship for grape anthocyanins. In addition and as a new insight, the copigmentation effects are carefully rationalized for the acylated anthocyanins.

## MATERIAL AND METHODS

### Experimental data

The grape anthocyanin spectra were collected from our database of HPLC chromatograms obtained in 2008, within the framework of the study on competitive copigmentation interactions (Rustioni, Bedgood Jr, Failla, Prenzler & Robards, 2012). Anthocyanins were extracted from the skin of Shiraz and Sangiovese berries. The primary pigment solutions were prepared after the careful removal of skin from 30 berries, and suspended in a 60 mL model-wine-buffer solution (12% ethanol and 2.5 g L<sup>-1</sup> tartaric acid adjusted at pH 3.3 with aqueous NaOH). The pigment extracts were obtained by filtration after this mixture was shaken for 6 hours. The extracts were characterized on a Varian Prostar 240I HPLC (Mulgrave, Vic, Australia) using a Phenomenex Gemini 5  $\mu$ m C18 110A 250 x 4.6 mm column (Lane Cove, NSW, Australia), with a Phenomenex SecurityGuard column, operated at 25°C. For the HPLC separation the mobile phase was water:formic acid:acetonitrile (87:10:3 v/v/v, eluent A; 40:10:50 v/v/v, eluent B), and the following gradient sequence was used: from 10 to 25% B (10 min), from 25 to 31% B (5 min), from 31 to 40% B (5 min), from 40 to 50% B (10 min), from 50 to 100% B (10 min) from 100 to 10% B (5 min), as previously described by Kammerer et al. (Kammerer, Claus, Carle & Schieber, 2004). The flow rate was 0.8 mL min<sup>-1</sup>. The eluent was monitored by a Varian Prostar 335 photodiode array detector (Mulgrave, Vic, Australia). Peak identification was achieved using both the retention time and the LCMS analysis as previously described (Rustioni, et al., 2012).

Malvidin aglycone, and caffeic and *p*-coumaric acids (SIGMA-ALDRICH) were used without further purification. To compare their spectra with those obtained in HPLC, three solutions (10 mg L<sup>-1</sup> for malvidin, 5.7 mg L<sup>-1</sup> for caffeic acid and 3.2 mg L<sup>-1</sup> for *p*-coumaric acid) were prepared using the same solvent as for the HPLC elution (water:formic acid:acetonitrile 65:10:25 v/v/v). A Jasco 7800 UV-Vis spectrophotometer was used to record absorption spectra from 200 to 600 nm.

Considering the high percentage of formic acid providing pH ca. 1.6, the flavylum cation form of the anthocyanins is unambiguously predominant. For this reason and for the sake of comparison with experimental data, all the theoretical calculations were performed considering this cationic form.

### Theoretical methodology

Over the past decade, the density functional theory (DFT) has been validated and extensively used to evaluate conformational, electronic and optical properties of natural polyphenols (Anouar, Gierschner, Duroux & Trouillas, 2012; Trouillas, Marsal, Siri, Lazzaroni & Duroux, 2006). TD-DFT turned out to be an accurate theoretical method to describe excited states and consequently UV/Visible properties at an acceptable computational time for medium-size polyphenols, namely containing up to 200 atoms (Anouar, et al., 2012; Nave, et al., 2012).

Hybrid functionals succeeded at describing most of polyphenol properties; the B3P86 functional has appeared particularly adapted to assess both their thermodynamic (Trouillas, et al., 2006) and UV/Visible absorption properties (Anouar, et al., 2012). Using the Pople-type triple- $\zeta$  basis set, TD-B3P86/6-311+G(d,p) allowed to establish reliable structure property (UV/Visible absorption) relationships for large series of polyphenols, at a reasonable computational time (Anouar, et al., 2012; Millot, Di Meo, Tomasi, Boustie & Trouillas, 2012).



B3P86 was thus extrapolated for the present work to evaluate both conformation and UV/Visible absorption properties of peonidin, cyanidin, malvidin, petunidin and delphinidin and their glucoside derivatives (Fig. 1).

Concerning the acylated derivatives, cofacial (non-covalent) intra-molecular interactions were examined between the anthocyanidin and the phenolic acyl (*i.e.*, *p*-coumaroyl and caffeoyl) moieties. It is well described that classical hybrid functionals fail at describing these non-covalent interactions, which are mainly dispersive effects (*e.g.*,  $\pi$ -stacking,  $\nu$ - $\pi$  and long-distance H-bonds). The empirical dispersion-corrected DFT (DFT-D) is a successful approach to evaluate these non-covalent complexation, also allowing to circumvent the use of high-costing post-HF methods (Grimme, 2006). Our recent parameterization of the B3P86-D2 functional provided very reliable results to describe non-covalent interaction in polyphenols and copigmentation (anthocyanidin:flavonol) complexes with respect to both post-HF methods and experiments (Di Meo, et al., 2012). Therefore in the present work, the ground state geometries of the acylated derivatives were corrected according to this empirical dispersion correction. The cc-pVDZ basis set was used, which has appeared sufficient to reach accuracy, with respect to high-level quantum calculations and experimental data, in the description of anthocyanidin:flavonol complexation.<sup>1</sup> All DFT-D calculations were achieved within the resolution of identity (RI) approximation, dramatically decreasing the computational time with a negligible error (Neese, Wennmohs, Hansen & Becker, 2009). When working with DFT-D(B3P86-D2), the geometries were obtained with the ORCA package (Neese, 2012). In the other case *i.e.*, when working with B3P86 (no dispersion correction), the geometries were calculated with GAUSSIAN09 (Frisch, et al., 2009). All TD-DFT calculations were achieved with GAUSSIAN09.

---

<sup>1</sup> It must be stressed that dispersion-corrected B3P86-D2 functional has been assessed and validated within double-z basis set precision.

Solvent effects were taken into account using implicit solvent models, in which the solute is embedded in a shape-adapted cavity surrounded by a dielectric continuum. Even if they do not explicitly account for inter-molecular interaction between solute and solvent, implicit solvent models have allowed reaching accuracy to evaluate various properties of polyphenols, including optical properties (Anouar, et al., 2012; Millot, et al., 2012). The qualitative description of the influence of solvent polarity is particularly relevant, which perfectly reproduce structure-property relationships. Methanol ( $\epsilon = 32.61$ ) was used to simulate the polarity of the experimental conditions used to measure the UV/Visible spectra. The conductor-like screening model (COSMO) (Sinnecker, Rajendran, Klamt, Diedenhofen & Neese, 2006) and the integral-equation formalism polarizable continuum model (IEFPCM) (Cossi, Scalmani, Rega & Barone, 2002) were used with ORCA and GAUSSIAN09, respectively.

## RESULTS AND DISCUSSION

### UV/Visible absorption properties of grape 3-*O*-glucosylated anthocyanins

The experimental spectra measured for the five 3-*O*-glucosylated anthocyanidins (compounds **1-5** namely cyanidin 3-*O*-glucoside, peonidin 3-*O*-glucoside, delphinidin 3-*O*-glucoside, petunidin 3-*O*-glucoside and malvidin 3-*O*-glucoside – also called oenin – as seen in Fig. 1), synthesized in grape berries, consist of three main peaks experimentally located at around i) 520 nm (Band I), ii) 440 nm (Band II) and iii) 330 nm (Band III) (Fig. 2a). The disubstituted B-ring compounds (*i.e.*, cyanidin 3-*O*-glucoside and peonidin 3-*O*-glucosides) have an additional absorption band located at around 375 nm (Band II<sub>b</sub>).

*Molecular orbital rationalization of Band I* - The highest absorption wavelength  $\lambda_{max}$  corresponding to Band I of compounds **1-5** are 516, 517, 524, 526 and 527 nm, respectively

(Table 1). As already described for anthocyanidins, this wavelength is slightly underestimated by TD-DFT calculations when using standard hybrid functionals (Anouar, et al., 2012; Chai & Head-Gordon, 2008). This band corresponds to a transition from the ground state ( $S_0$ ) to the first excited state ( $S_1$ ) and is mainly assigned to the HOMO (highest occupied molecular orbital) to LUMO (lowest unoccupied molecular orbital) electronic transition.<sup>2</sup> In order to simplify notations, the HOMO→LUMO electronic transition is quoted H→L throughout the text. Both molecular orbitals (MO) are delocalized over the whole anthocyanidin moiety (Fig. 3a&b). This allows an efficient overlap between the two molecular orbitals involved in the transition, which provides relatively high oscillator strengths (and therefore high absorption intensities) for all five compounds ( $f$  around 0.60 as seen in Table 1).

The compounds having a tri-substituted B-ring (compounds **3-5**), exhibit a (red)-bathochromic shift compared to the di-substituted (**1** and **2**) derivatives (Fig. 2a). This is attributed to the (+M) mesomeric effect that slightly but significantly extends  $\pi$ -conjugation in the B-ring, which subsequently lowered the H-L gap ( $\Delta E_{\text{gap}}$ , Fig. 3a&b). When adding one OH group (*i.e.*, compounds **1** vs. **3** and **2** vs. **4**), both H and L are stabilized but to a lower extent for H, thus decreasing the gap (*e.g.*,  $\Delta E_{\text{gap}}$  decreases from 2.91 to 2.86 eV, from **1** to **3**, see Fig. 3a&b). Such an effect was similarly observed for aglycone flavonoids.(Anouar, et al., 2012) When replacing an OH group by an OMe group, both frontier MOs are destabilized, but the H orbital is more impacted by this destabilization, resulting in the decrease of the H-L gap (*e.g.*,  $\Delta E_{\text{gap}}$  is 2.86 and 2.75 eV for **3** and **5**, respectively, see S1).

The theoretical excited states of the aglycone counterpart of compounds **1-5** were also evaluated for the sake of comparison. From this comparison, it appears that the sugar moiety

<sup>2</sup> In the present work, the orbital analysis is based on the 3D distribution of only the main two MO involved in the main electronic transition. The full analysis taking the contributions of all electronic transitions into account was also achieved (see Supplement Information). However, this latter (thorough) analysis does not influence the conclusions (except concerning one point, which is mentioned in the next footnote); thus for the sake of simplicity, the simpler analysis is kept in the main body of the text.

creates new MOs lying below H-4 (see Supplementary Information), which do not directly influence the absorption spectra *e.g.*, by the formation of new bands. However, the sugar addition induces a slight increase of the H-L gap, due to both the stabilization of H and destabilization of L. This is in agreement with experimental data, as it results in a significant hypsochromic shift of Band I in the glucosides' spectra (*e.g.*,  $\lambda_{max}$  equal 527 and 536 nm for compound **5** and its aglycone counterpart, respectively as seen in Fig. 2b). This does not influence the global spectra, which are similar in shape with both forms.

*Molecular orbital rationalization of Band II* - Band II appears in the experimental spectra as a shoulder of the maximum absorption band, which is located at around 440 nm (Fig. 2a). It corresponds to the second excited state ( $S_2$ ) and is mainly assigned to the H-1 $\rightarrow$ L and H-2 $\rightarrow$ L for di-substituted (*i.e.*, compounds **1** and **2**) and tri-substituted (*i.e.*, compounds **3-5**) compounds, respectively (Table 1). L being delocalized on the A and C rings, this shoulder appears attributed to this moiety. A thorough analysis of the MO spatial distribution highlights interconversion between both H-1 and H-2 for the di- and tri-substituted compounds; that is, the spatial distribution of H-1 in the di-substituted compound is similar to that of H-2 in the tri-substituted compound (Fig. 3a&b). These MOs are delocalized over the entire anthocyanidin moiety. Moreover, they exhibit the same energy (*ca.* -7.75 eV for all compounds, as seen in Supplementary Information). For the tri-substituted compounds, H-1 is delocalized over the B-ring only. This MO slightly contributes to other excited states, including  $S_1$  (data not shown).

For the di-substituted compounds (**1** and **2**), there exists a specific absorption band, quoted Band II<sub>b</sub> in Table 1, which is absent in the experimental spectra of the tri-substituted compounds (**3**, **4** and **5**). Quantum chemistry calculations fully rationalize this experimentally observed difference. Band II<sub>b</sub> is assigned to the H-2 $\rightarrow$ L electronic transition. In the di-substituted compounds, H-2 is slightly delocalized on the A&C-rings (Fig. 3a), allowing

electronic transitions with low oscillator strengths ( $f = 0.15$  and  $0.18$  for **1** and **2**, respectively). In the tri-substituted compounds, due to the MO redistribution described above, H-1 is almost fully delocalized on the B-ring, preventing this electronic transition involving the A&C-rings. Moreover, in this case, the energetic difference between H-1 and L is lowered. Thus for the tri-substituted compounds, Band II<sub>b</sub> is weak and red-shifted; it cannot be experimentally observed under classical conditions (i.e., room temperature and classical resolutions).

*Molecular orbital rationalization of Band III* - Band III is mainly assigned to the H-4→L electronic transition. In agreement with the experimental data, Band III exhibits relatively low oscillator strengths compare to those of Band I, for all five compounds ( $f$  is ranging from 0.02 to 0.08, see Table 1). The (blue)hypsochromic shift experimentally observed from the tri- to the di-substituted compounds (e.g.,  $\lambda = 348$  and  $328$  nm for **5** and **1**, respectively, see Table 1) is rationalized by the influence of the sugar moiety, which surprisingly, but in full agreement with the experimental data, borrows part of the H-4 orbital, in the di-substituted compounds (Fig. 3a&b). In this case the sugar moiety stabilizes H-4, thus increasing the energy difference between H-4 and L, inducing the hypsochromic shift. This is probably only an (energetic) indirect effect, as the electronic excitation does not involve the sugar moiety (Fig. S2).<sup>3</sup>

#### UV/Visible absorption properties of grape acylated anthocyanins

The spectral modulation related to esterification is discussed for the malvidin derivatives, as they are the main grape anthocyanidins.

<sup>3</sup> This is clearly observed when analyzing all MO involved in this electronic transition.

*Conformational analysis* - Concerning the three malvidin 3-*O*-glucoside esters (compounds **6**, **7** and **8**, see Fig. 1) one, two (**7A** and **7B**) and two (**8A** and **8B**) conformers were obtained, respectively (Fig. 4).

For each possible conformer, the Boltzmann distribution percentages  $D_{\text{Bolt}}$  were estimated (Table 2) from the relative energies  $\Delta E_{\text{relative}}$  (as calculated between all conformers with B3P86-D2/cc-pVDZ), according to the following formula:

$$D_{\text{Bolt}} = \exp\left(-\frac{\Delta E_{\text{relative}}}{RT}\right),$$

where  $R$  is the ideal gas constant and  $T$  equals 298 K.

The non-covalent intra-molecular interactions between the acyl and anthocyanidin moieties play a crucial role in the stabilization of these conformers. A strong H-bond (distance lower than 1.65 Å) between the 5-OH and the ester keto groups is observed in **6**, **7B**, **8A** and **8B** (Fig. 4). A weaker H-bond is observed between the 5-OH and the O atom involved in the esterification (distance of 2.39 Å) for **7A**. Other non-covalent interactions are observed in **7A**, **7B** and **8A** (Fig. 4), namely i) one H-bonding between the 7-OH and the 4''-OH groups (distance of 1.80 and 2.27 Å, respectively) for **7A** and **7B**, which is not present in compound **8** as 4''-OH is absent in this case, and ii)  $\pi$ -stacking interaction in **7B** and **8A** (distance of 4.20 Å).

The conformation populations of **7** and **8**, show a predominance of **7A** ( $D_{\text{Bolt}} = 90\%$ ) and **8A** ( $D_{\text{Bolt}} = 83\%$ ) for both compounds, respectively. This clearly suggests that both H-bonding and  $\pi$ -stacking interactions are the driving forces of this intra-molecular folding.

*UV/Visible absorption spectra of 6, 7 and 8: a matter of intra-molecular copigmentation -*

When compared to the glycosylated malvidin (**5**), the experimental spectra of **6**, **7** and **8** clearly show the influence of esterification, mainly in the presence of the phenolic acid moiety

(compounds **7** and **8**). The three acylated anthocyanins exhibit an experimental bathochromic shift of Band I that is lower for **6** ( $\Delta\lambda_{max}$  around 2, 5 and 4 nm for **6**, **7** and **8**, respectively).

The bathochromic shift of Band I is mainly rationalized by  $\pi$ -stacking complexation. In conformations **7B** and **8A**, the maximum absorption wavelength (related to Band I) and other very close absorption wavelengths are assigned to the H $\rightarrow$ L and H-1 $\rightarrow$ L electronic transitions (Table 2a). In all conformers, H and L are mainly delocalized on the anthocyanin moiety (Fig. 3c-f), and the electron transition presents no charge-transfer character. In the particular case of conformers **7B** and **8A**, H is slightly located on the phenolic ring of the ester moiety (Fig. 3d&e). This can be better evaluated by the LCAO (linear combination of atomic orbital) coefficients, which reflect the atomic weight of a given MO. For H of **7B** and **8A**, these coefficients are 13% and 21% on the acyl moiety, respectively (Table S2). However, a detailed analysis of MO contributions (see Supplementary Information) shows that the esterification affects neither the spatial distribution nor the energy of H and L, showing that the bathochromic shift is not rationalized by the H $\rightarrow$ L contribution. The main contribution to the modification of the excited state (with respect to that of compound **5**) comes from H-1, which is highly delocalized over the phenolic ester moiety for all conformers of **7** and **8** (Fig. 3c-f). Therefore the H-1 $\rightarrow$ L electronic transition exists only because of the formation of a charge transfer excited state (CT-ES), inducing a global bathochromic shift attributed to esterification. In conformers **7B** and **8A**, H-1 is also located on the anthocyanin moiety (the LCAO coefficients of H are 57% and 49% on the anthocyanin moiety, for **7B** and **8A**, respectively see Table S2), which increases the corresponding oscillator strength (Table 2).

Compound **7** exhibits a slightly lower experimental bathochromic shift than **8** ( $\Delta\lambda_{max} = 4$  and 5 nm, for both compounds respectively, see Table 2a). In contrast, the theoretical bathochromic shift is higher with the former compound (**7**) i.e., 24.7 vs. 18.9 nm, for both compounds respectively (Table 2a). This is consistent with the higher electron donor capacity

of the ortho-dihydroxyphenyl (catechol) moiety. Thus the lower experimental bathochromic shift observed for **7** is attributed to a lower population of the  $\pi$ -stacked conformation (**7B**) in solution compared to that of **8** (**8A**). This highlights the importance of i) charge-transfer in the excited state and ii) populations for all the possible copigmentation complexes, as already shown in our previous work (Di Meo, et al., 2012).

*A new band (III<sub>b</sub>) at 330 nm* - The acylated compounds exhibit a new absorption band, quoted Band III<sub>b</sub>, experimentally located at around 330 nm (Fig. 2c), which is somehow a modulation of Band III. This band is actually the sum of the minor anthocyanic absorption Band III (Table 1 and Fig. 2a) and the (red)bathochromic-shifted band mainly attributed to the stand-alone phenolic acid (*e.g.*,  $\lambda = 324$  and  $336$  nm for caffeic acid and the caffeoyl ester of malvidin 3-*O*-glucoside, respectively and  $\lambda = 309.6$  and  $316$  nm for *p*-coumaric acid and the *p*-coumaroyl ester of malvidin 3-*O*-glucoside, respectively, see Table 2b and Fig. 2c). It is theoretically assigned to several contributions predominantly H-1 $\rightarrow$ L+1, H-4/5/6 $\rightarrow$ L and H $\rightarrow$ L+2 electronic transitions (Table 2b). The first contribution is purely attributed to the phenol acid moiety, both MO being delocalized on this moiety. These MO are stabilized in the presence of the anthocyanin moiety, H being more stabilized than L, which should induce a hypsochromic shift. The global bathochromic shift is due to the other two contributions. Among these contributions, the H-4 $\rightarrow$ L contribution corresponds to that already observed for compound **5**, as the main contribution of Band III.

## CONCLUSION

Grapes and wines represent agricultural product of utmost importance in food industry. The color of the final product is a major descriptor of quality. A deep understanding of the optical properties of the main *Vitis vinifera* L. pigments represents an effective support for the



industries to address market requirements. This is mandatory to develop new analytical methods based on the optical properties and to deeply understand fruit potential. As described above, quantum chemistry calculations have allowed elucidating the structure (optical) properties of a series of grape pigments. These calculations provide a molecular picture of the pigments as well as a molecular orbital description of the excited states related to the different absorption bands responsible for color. Subtle effects such as copigmentation can also be explained by using the adapted theoretical methodologies, namely DFT-D. All the theoretical data support the experimental observations. The full MO description of light absorption, in the visible range, enables to tune optical properties (according to the chemical structures of the different grape pigments), and subsequently color variation. Quantum calculation can now be considered as a promising analytical tool for wine industry.

**ACKNOWLEDGEMENTS**

The authors acknowledge Prof. Paul Prenzler (School of Agricultural and Wine Sciences, Charles Sturt University, Wagga Wagga, NSW, Australia) for the availability to share the HPLC results.

The authors thank the French embassy for the financial support in the framework of the “Borse di ricerca scientifica dell’Ambasciata di Francia” project; the “Conseil Régional du Limousin” for financial support and CALI (CALcul en LIMousin) for computing facilities. Research in Limoges is also supported by the COST action CM0804 “Chemical Biology with Natural Compounds”. The authors gratefully acknowledge the support by the Operational Program Research and Development for Innovations–European Regional Development Fund (project CZ.1.05/2.1.00/03.0058 of the Ministry of Education, Youth and Sports of the Czech Republic). Research in Mons is supported by BELSPO (PAI 7/05), Région Wallonne (OPTI2MAT Excellence program) and FNRS-FRFC.

This work is a joint publication of the COST Action FA1003 “East-West Collaboration for Grapevine Diversity Exploration and Mobilization of Adaptive Traits for Breeding”.

370 **TABLES**

371 **Table 1.** Theoretical excitation energies (E, eV), absorption wavelengths ( $\lambda$ , nm), oscillator  
 372 strengths ( $f$ ), main electronic transition contribution and experimental absorption wavelength  
 373 ( $\lambda_{exp}$ , nm) of anthocyanidin 3-*O*-glucosides. The calculations (excited states + geometries)  
 374 were performed with IEFPCM-B3P86/6-311+G(d,p).  
 375

Band	Compound	E	$\lambda$	$f$	Electronic transition contribution	$\lambda_{exp}$
I	<b>1</b>	2.59	478.0	0.58	H→L (67%)	516
	<b>2</b>	2.57	482.8	0.59	H→L (68%)	517
	<b>3</b>	2.57	482.8	0.57	H→L (67%)	524
	<b>4</b>	2.56	483.4	0.61	H→L (68%)	526
	<b>5</b>	2.49	497.1	0.59	H→L (68%)	527
II	<b>1</b>	2.95	419.8	0.07	H-1→L (67%)	~440
	<b>2</b>	2.92	424.8	0.03	H-1→L (68%)	~440
	<b>3</b>	2.95	420.1	0.11	H-2→L (67%)	~440
	<b>4</b>	2.93	423.7	0.06	H-2→L (67%)	~440
	<b>5</b>	2.92	424.0	0.05	H-2→L (68%)	~440
II <sub>b</sub>	<b>1</b>	3.23	384.0	0.15	H-2→L (70%)	373
	<b>2</b>	3.22	385.2	0.18	H-2→L (69%)	375
	<b>3</b>	2.68	463.2	0.03	H-1→L (70%)	-
	<b>4</b>	2.70	456.0	0.01	H-1→L (70%)	-
	<b>5</b>	2.68	461.9	0.07	H-1→L (70%)	-
III	<b>1</b>	3.88	319.5	0.02	H-4→L (62%)	328
	<b>2</b>	3.88	319.8	0.02	H-4→L (62%)	328
	<b>3</b>	3.73	332.2	0.06	H-4→L (66%)	346
	<b>4</b>	3.72	332.9	0.08	H-4→L (66%)	347
	<b>5</b>	3.69	336.2	0.08	H-4→L (66%)	348

376

**Table 2.** Theoretical excitation energies ( $E$ , eV), absorption wavelengths ( $\lambda$ , nm), oscillator strengths ( $f$ ), electronic transition contribution and experimental absorption wavelength ( $\lambda_{exp}$ , nm) of the different optimized conformation of acetyl (**6**), caffeoyl (**7**) and *p*-coumaroyl (**8**) esters of malvidin 3-*O*-glucoside, and related theoretical and experimental bathochromic shifts ( $\Delta\lambda_{th}$  and  $\Delta\lambda_{exp}$ , nm) concerning (a) Band I and (b) Band III. Boltzmann distributions  $D_{Boltz}$  are expressed in %. The calculations were performed with IEFPCM-B3P86/6-311+G(d,p)//COSMO-B3P86(D2)/cc-pVDZ.

(a)

Ester	Conformation	$D_{Boltz}$	$E$	$\lambda$	$f$	Electronic transition contribution	$\Delta\lambda_{th}^a$	Exp	
								$\lambda_{exp}$	$\Delta\lambda_{exp}^a$
Acetic ester	<b>6</b>	90%	2.51	494.9	0.58	H→L (68%)	-2.2	529	2
Caffeoyl ester	<b>7A</b>	90%	2.47	502.2	0.17	H-1→L (57%)	5.0	531	4
						H→L (40%)			
			2.50	496.5	0.38	H→L (54%)	-0.6		
	<b>7B</b>	6%	2.38	521.8	0.10	H-1→L (52%)	24.7		
			2.49	498.1	0.37	H-1→L (46%)	1.0		
						H→L (49%)			
<i>p</i> -Coumaroyl ester	<b>8A</b>	83%	2.40	516.0	0.41	H→L (66%)	18.9	532	5
			2.59	479.5	0.03	H-1→L (58%)			
	<b>8B</b>	15%	2.50	495.2	0.57	H→L (67%)	-1.9		

<sup>a</sup> the shift is performed with respect to malvidin 3-*O*-glucoside  $\lambda_{max}$ .

(b)

Ester	Conformation	$D_{boltz}$	$E$	$\lambda$	$f$	Electronic transition contribution	$\Delta\lambda_{th}$	Exp	
								$\lambda_{exp}$	$\Delta\lambda_{exp}$
Acetic ester	<b>6</b>	100	3.64	340.8	0.07	H-3→L (65%)	nd	348	nd
Caffeoyl ester	<b>7A</b>	90%	3.66	339.1	0.03	H-5→L (48%)	1.1	324	12
						H-6→L (36%)			
						H-1→L+1 (31%)			
						H→L+2 (15%)			
	<b>7B</b>	6%	3.72	333.5	0.64	H-1→L+1 (62%)	-4.5		
			3.51	353.7	0.32	H-1→L+1 (68%)	15.7		
						H-4→L+1 (10%)			
<i>p</i> -Coumaroyl ester	<b>8A</b>	83%	3.64	340.5	0.03	H-5→L (65%)	2.5	316	6
			3.68	336.6	0.25	H-1→L+1 (55%)	19.6		
						H-5→L (33%)			
			3.74	331.5	0.22	H-5→L (47%)	14.5		
	<b>8B</b>	15%				H-1→L+1 (34%)			
						H→L+2 (15%)			
			3.70	334.8	0.68	H-1→L+1 (64%)	17.7		
						H-4→L+1 (14%)			
			3.75	331.1	0.13	H-6→L (62%)	14.0		
						H-4→L (20%)			
						H-1→L+1 (19%)			
						H-6→L (15%)			

387 <sup>a</sup> the shift is performed with respect to the stand-alone acid  $\lambda_{\max}$  (i.e., caffeic or p-coumaric acid in solution).

ACCEPTED MANUSCRIPT

## REFERENCES

- Allen, M. (1998). Phenolics and Extraction. In A. S. o. V. a. Oenology (Ed.), *Proceedings ASVO*, Accepted). Adelaide.
- Anouar, E. H., Gierschner, J., Duroux, J.-L., & Trouillas, P. (2012). UV/Visible spectra of natural polyphenols: A time-dependent density functional theory study. *Food Chemistry*, *131*, 79-89.
- Castañeda-Ovando, A., Pacheco-Hernández, M. d. L., Páez-Hernández, M. E., Rodríguez, J. A., & Galán-Vidal, C. A. (2009). Chemical studies of anthocyanins: A review. *Food Chemistry*, *113*, 859-871.
- Chai, J.-D., & Head-Gordon, M. (2008). Long-range corrected hybrid density functionals with damped atom-atom dispersion corrections. *Physical Chemistry Chemical Physics*, *10*, 6615-6620.
- Cossi, M., Scalmani, G., Rega, N., & Barone, V. (2002). New developments in the polarizable continuum model for quantum mechanical and classical calculations on molecules in solution. *Journal of Chemical Physics*, *117*, 43-54.
- Dallas, C., & Laureano, O. (1994). Effect of SO<sub>2</sub> on the extraction of individual anthocyanins and colored matter of three Portuguese grape varieties during winemaking. *Vitis*, Accepted.
- Dangles, O., Saito, N., & Brouillard, R. (1993). Anthocyanin intramolecular copigment effect. *Phytochemistry*, *34*, 119-124.
- Di Meo, F., Sancho Garcia, J. C., Dangles, O., & Trouillas, P. (2012). Highlights on Anthocyanin Pigmentation and Copigmentation: A Matter of Flavonoid  $\pi$ -Stacking Complexation To Be Described by DFT-D. *Journal of Chemical Theory and Computation*, *8*, 2034-2043.

- 412 Ferrandino, A., Guidoni, S., & Mannini, F. (2007). Grape quality parameters and  
413 polyphenolic content of different ‘Barbera’ and ‘Nebbiolo’ (*Vitis vinifera* L.) clones as  
414 influenced by environmental conditions – preliminary results. *Acta Horticulturae*, 754,  
415 437-442.
- 416 Fischer, U., Löchner, M., & Wolz, S. (2006). Red Wine Authenticity: Impact of  
417 Technology on Anthocyanin Composition. In *Authentication of Food and Wine*, vol. 952  
418 (pp. 239-253): American Chemical Society.
- 419 Frisch, M. J., Trucks, G. W., Schlegel, H. B., Scuseria, G. E., Robb, M. A., Cheeseman, J.  
420 R., Scalmani, G., Barone, V., Mennucci, B., Petersson, G. A., Nakatsuji, H., Caricato, M.,  
421 Li, X., Hratchian, H. P., Izmaylov, A. F., Bloino, J., Zheng, G., Sonnenberg, J. L., Hada,  
422 M., Ehara, M., Toyota, K., Fukuda, R., Hasegawa, J., Ishida, M., Nakajima, T., Honda, Y.,  
423 Kitao, O., Nakai, H., Vreven, T., Montgomery, J. A., Peralta, J. E., Ogliaro, F., Bearpark,  
424 M., Heyd, J. J., Brothers, E., Kudin, K. N., Staroverov, V. N., Kobayashi, R., Normand, J.,  
425 Raghavachari, K., Rendell, A., Burant, J. C., Iyengar, S. S., Tomasi, J., Cossi, M., Rega,  
426 N., Millam, J. M., Klene, M., Knox, J. E., Cross, J. B., Bakken, V., Adamo, C., Jaramillo,  
427 J., Gomperts, R., Stratmann, R. E., Yazyev, O., Austin, A. J., Cammi, R., Pomelli, C.,  
428 Ochterski, J. W., Martin, R. L., Morokuma, K., Zakrzewski, V. G., Voth, G. A., Salvador,  
429 P., Dannenberg, J. J., Dapprich, S., Daniels, A. D., Farkas, Foresman, J. B., Ortiz, J. V.,  
430 Cioslowski, J., & Fox, D. J. (2009). Gaussian 09, Revision A.02. In, citeulike-article-  
431 id:9096580). Wallingford CT.
- 432 García-Puente Rivas, E., Alcalde-Eon, C., Santos-Buelga, C., Rivas-Gonzalo, J. C., &  
433 Escribano-Bailón, M. T. (2006). Behaviour and characterisation of the colour during red  
434 wine making and maturation. *Analytica Chimica Acta*, 563, 215-222.
- 435 Grimme, S. (2006). Semiempirical GGA-type density functional constructed with a long-  
436 range dispersion correction. *Journal of Computational Chemistry*, 27, 1787-1799.

- Kammerer, D., Claus, A., Carle, R., & Schieber, A. (2004). Polyphenol Screening of Pomace from Red and White Grape Varieties (*Vitis vinifera* L.) by HPLC-DAD-MS/MS. *Journal of Agricultural and Food Chemistry*, 52, 4360-4367.
- Kennedy, J. A., Saucier, C., & Glories, Y. (2006). Grape and Wine Phenolics: History and Perspective. *American Journal of Enology and Viticulture*, 57, 239-248.
- Mattivi, F., Guzzon, R., Vrhovsek, U., Stefanini, M., & Velasco, R. (2006). Metabolite Profiling of Grape: Flavonols and Anthocyanins. *Journal of Agricultural and Food Chemistry*, 54, 7692-7702.
- Millot, M., Di Meo, F., Tomasi, S., Boustie, J., & Trouillas, P. (2012). Photoprotective capacities of lichen metabolites: A joint theoretical and experimental study. *Journal of Photochemistry and Photobiology B: Biology*, 111, 17-26.
- Nave, F., Brás, N. F., Cruz, L., Teixeira, N., Mateus, N., Galembeck, S. E., Di Meo, F., Trouillas, P., Dangles, O., & De Freitas, V. (2012). The influence of a flavan-3-olic substituent in the copigmentation ability of anthocyanins towards vinylcatechin dimers and procyanidins. *Journal of Physical Chemistry B*, 116, 14089-14099.
- Neese, F. (2012). The ORCA program system. *Wiley Interdisciplinary Reviews: Computational Molecular Science*, 2, 73-78.
- Neese, F., Wennmohs, F., Hansen, A., & Becker, U. (2009). Efficient, approximate and parallel Hartree-Fock and hybrid DFT calculations. A 'chain-of-spheres' algorithm for the Hartree-Fock exchange. *Chemical Physics*, 356, 98-109.
- Roggero, J. P., Coen, S., & Ragonnet, B. (1986). High Performance Liquid Chromatography Survey on Changes in Pigment Content in Ripening Grapes of Syrah. An Approach to Anthocyanin Metabolism. *American Journal of Enology and Viticulture*, 37, 77-83.



- 461 Rustioni, L., Basilico, R., Fiori, S., Leoni, A., Maghradze, D., & Failla, O. (2013). Grape  
462 Colour Phenotyping: Development of a Method Based on the Reflectance Spectrum.  
463 *Phytochemical Analysis*, 10.1002/pca.2434.
- 464 Rustioni, L., Bedgood Jr, D. R., Failla, O., Prenzler, P. D., & Robards, K. (2012).  
465 Copigmentation and anti-copigmentation in grape extracts studied by spectrophotometry  
466 and post-column-reaction HPLC. *Food Chemistry*, 132, 2194-2201.
- 467 Rustioni, L., Rossoni, M., Calatroni, M., & Failla, O. (2011). Influence of bunch exposure  
468 on anthocyanins extractability from grapes skins (*Vitis vinifera* L.). *Vitis*, 50, 137-143.
- 469 Rustioni, L., Rossoni, M., Cola, G., Mariani, L., & Failla, O. (2011). Bunch exposure to  
470 direct solar radiation increases ortho-diphenol anthocyanins in Northern Italy climatic  
471 condition. *Journal International des Sciences de la Vigne et du Vin*, 45, 85-99.
- 472 Rustioni, L., Rossoni, M., Failla, O., & Scienza, A. (2013). Anthocyanin esterification in  
473 Sangiovese grapes. *Italian Journal of Food Science*, 25, 133-141.
- 474 Sinnecker, S., Rajendran, A., Klamt, A., Diedenhofen, M., & Neese, F. (2006). Calculation  
475 of Solvent Shifts on Electronic g-Tensors with the Conductor-Like Screening Model  
476 (COSMO) and Its Self-Consistent Generalization to Real Solvents (Direct COSMO-RS).  
477 *Journal of Physical Chemistry A*, 110, 2235-2245.
- 478 Trouillas, P., Marsal, P., Siri, D., Lazzaroni, R., & Duroux, J. L. (2006). A DFT study of  
479 the reactivity of OH groups in quercetin and taxifolin antioxydants : The specificity of the  
480 3-OH site. *Food Chemistry*, 97, 10.

## FIGURE CAPTIONS

**Figure 1.** Chemical structures of the five glucosylated (a) and three acylated (b) studied anthocyanins.

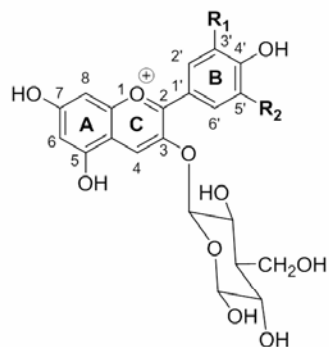
**Figure 2.** Experimental spectra of (a) anthocyanidin 3-*O*-glucosides (compounds **1-5**); (b) malvidin aglycone and malvidin 3-*O*-glucoside (**5**); and (c) malvidin 3-*O*-glucoside (**5**), oenin esters (compounds **7** and **8**), and relative phenolic acids.

All the spectra are normalized to appear in at a similar scale: anthocyanic molecules are normalized at a relative absorption value of 100 in the main peak (ca. 530 nm); phenolic acids are normalized according to the corresponding ester (ca. 330 nm).

**Figure 3.** Molecular orbital (MO) diagrams of the di-substituted (a) compound **1** and (b) tri-substituted compound **3** and the different conformations of compounds **7** and **8**: (c) **7A** (d) **7B**, (e) **8A** and (f) **8B**. The anthocyanidin moiety is in red, the sugar moiety is in blue and the acyl moiety is in green. The calculations were performed with IEFPCM-B3P86/6-311+G(d,p) and IEFPCM-B3P86/6-311+G(d,p)//COSMO-B3P86(D2)/cc-pVDZ with **1&3** and **7&8**, respectively.

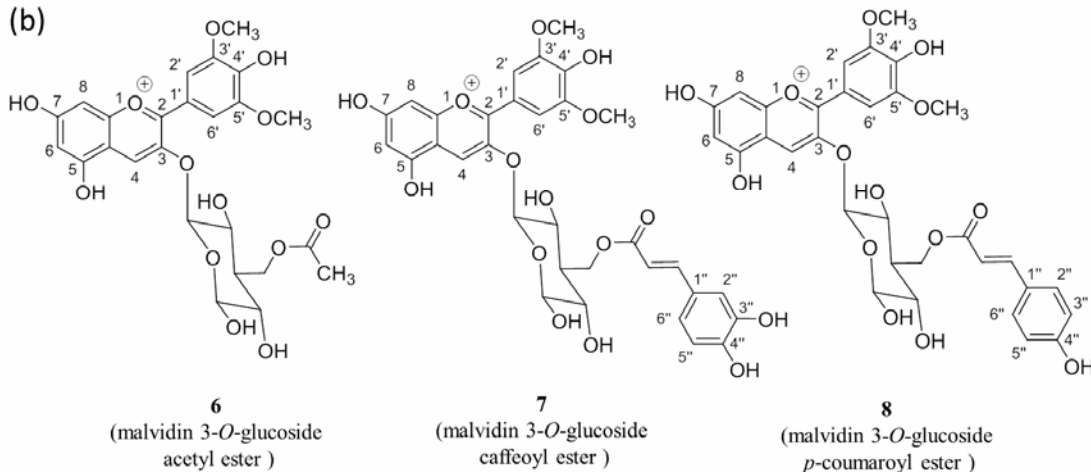
**Figure 4.** Optimized geometries of the acetyl ester (**6**), caffeic ester (**7A**; **7B**) and p-coumaric ester (**8A**; **8B**) of malvidin 3-*O*-glucoside; the anthocyanidin, sugar and the acyl moieties are in red, blue and green, respectively. The most relevant non-covalent intra-molecular interactions between the acyl and anthocyanidin moieties are underlined by broken lines. The calculations were performed with IEFPCM-B3P86/6-311+G(d,p)//COSMO-B3P86(D2)/cc-pVDZ.

(a)

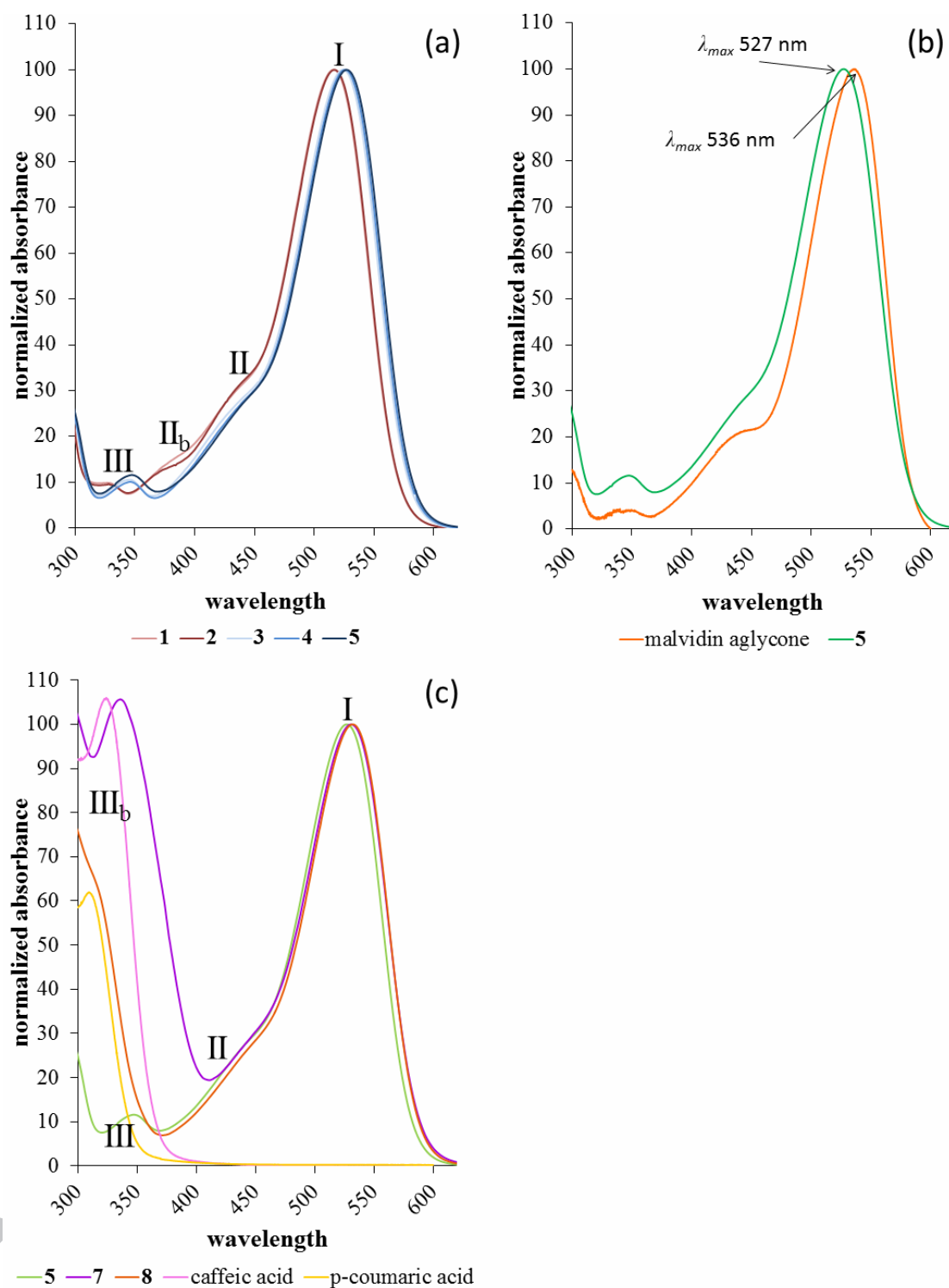


Compounds	Name	R <sub>1</sub>	R <sub>2</sub>
1	Cyanidin 3- <i>O</i> -glucoside	OH	H
2	Peonidin 3- <i>O</i> -glucoside	OMe	H
3	Delphinidin 3- <i>O</i> -glucoside	OH	OH
4	Petunidin 3- <i>O</i> -glucoside	OMe	OH
5	Malvidin 3- <i>O</i> -glucoside	OMe	OMe

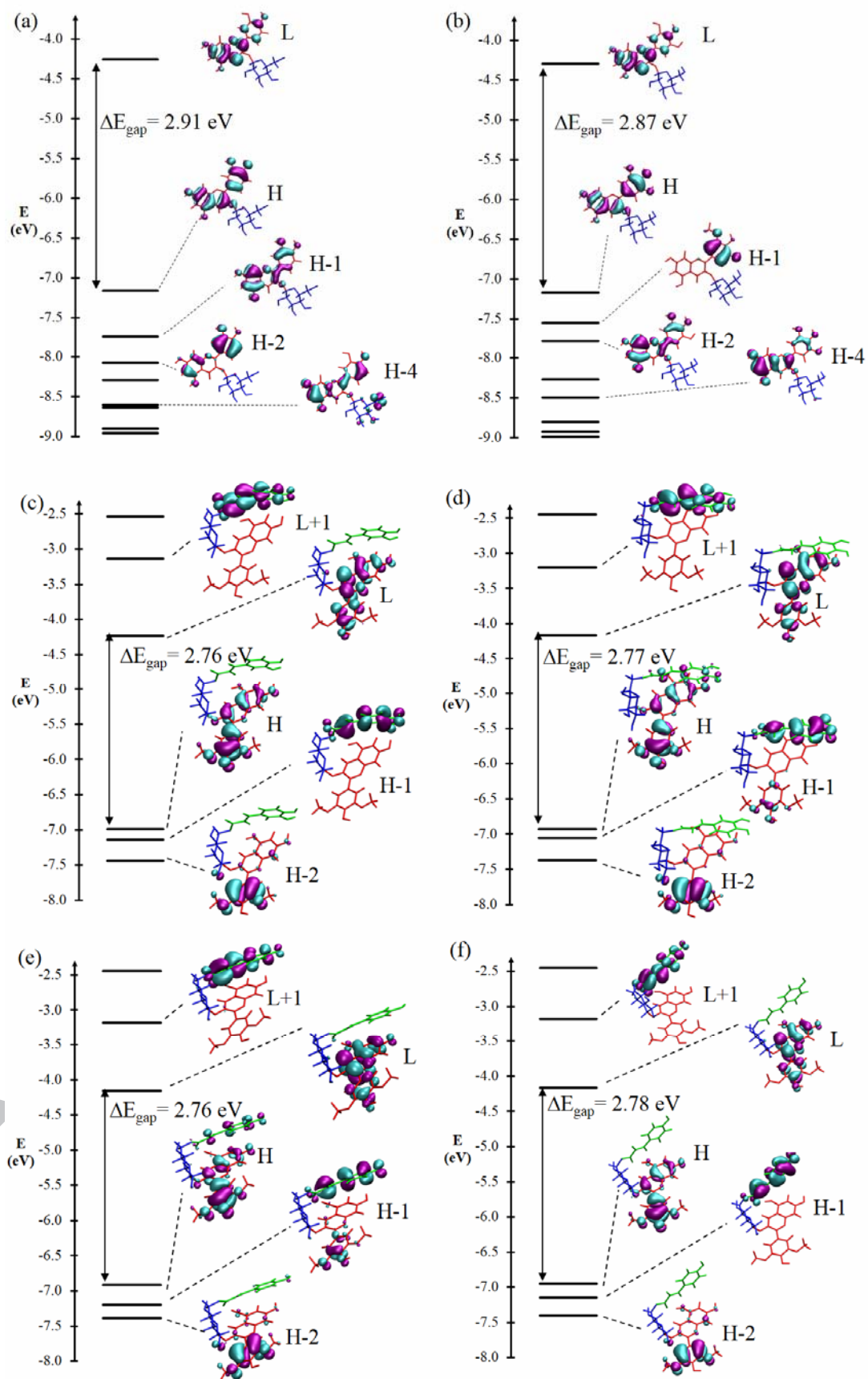
(b)

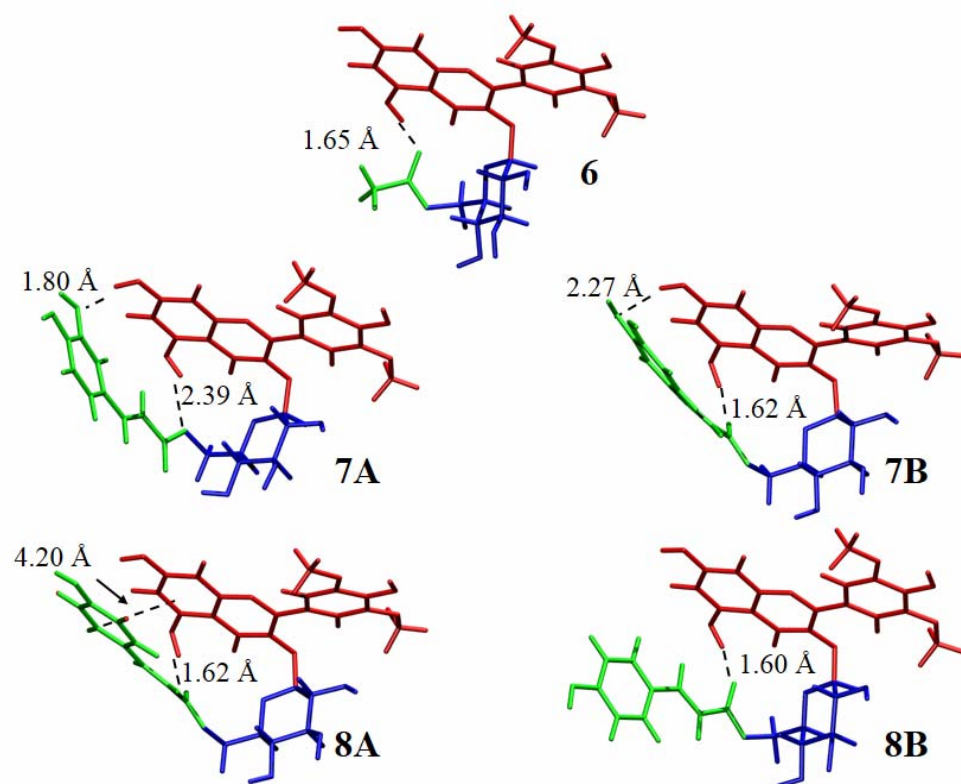


508



509





511

512 **HIGHLIGHTS:**

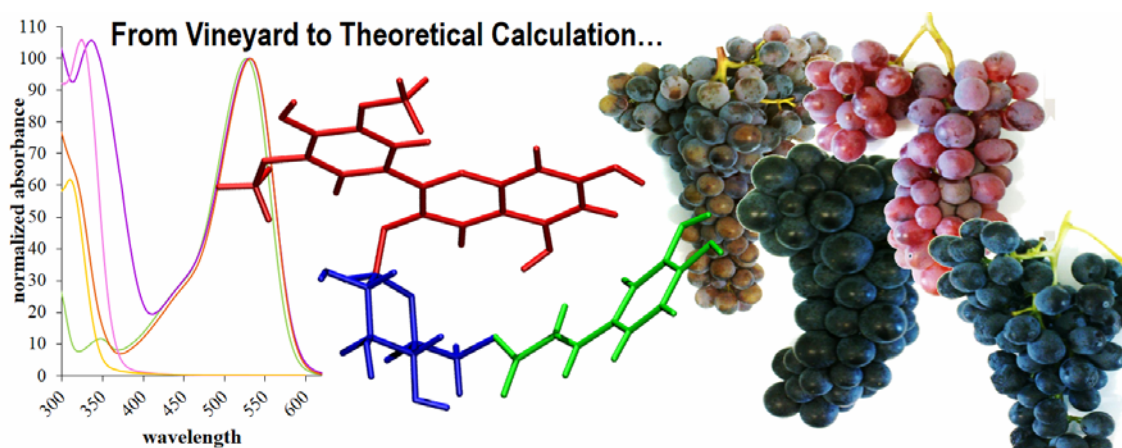
513 Grape anthocyanins colors were rationalized using quantum chemistry calculations.

514 Absorption differences related to pigment substitutions were explained.

515 Intramolecular copigmentation was rationalized for acylated pigments.

516

ACCEPTED MANUSCRIPT



517